NOISY NONLINEAR MOTIONS OF MOORED SYSTEM. II: EXPERIMENTAL STUDY

By S. C. S. Yim[1] and H. Lin[2]

ABSTRACT: An experimental study of a nonlinear moored structural system subjected to monochromatic wave excitations with random perturbations is reported in this paper. Sources of nonlinearity in the system include large geometric configurations and wave-induced quadratic drag. Random perturbations in the waves are approximated by linearly filtered white noise. An analytical model derived in Part I to assimilate the noisy nonlinear response is validated by good agreements shown in comparisons of simulated and experimental results in both time and frequency domains. System parameters of the analytical model are identified based on the experimental data. Noise effects on the nonlinear responses are examined. Experimental results indicate that the presence of random noise bridges the domains of multiple coexisting response attractors, and transitions among the multiple steady states are observed as analytically predicted in Part I.

INTRODUCTION

A wealth of complex nonlinear response behavior, including chaos, of ocean structural systems under deterministic monochromatic wave excitations has been studied analytically and demonstrated via computer simulations (Gottlieb and Yim 1992, 1993). Nonlinearities of the system are induced by a combination of geometrically nonlinear restoring force and (quadratic) drag force. In a deterministic setting, local and global stability analyses have been conducted, and stability regions of various nonlinear responses have been identified (Gottlieb and Yim 1992, 1993). A fine bifurcation superstructure is found (Gottlieb et al. 1997) and the sequential ordering indices imply the existence of higher order nonlinear responses (e.g., ultra-subharmonic and quasi-periodic) and possible routes to chaos.

In addition to the analytical and numerical investigations, experimental studies have also been conducted to verify the analytical predictions in deterministic settings (Yim et al. 1993). Nonlinear responses including subharmonics and ultraharmonics and bifurcations are observed experimentally. Underlying bifurcation superstructures are also detected, and the existence of higher order nonlinear responses (e.g., quasi-periodic and chaotic) is indicated. Despite good agreements between numerical predictions and experimental results, there are experimental observations that cannot be explained using only deterministic analysis procedures (Yim et al. 1993), such as an "unexpected" transition from (transient) harmonic to (steady-state) subharmonic observed in a sample experimental response [cf. Fig. 1 in Part I, Lin and Yim (1997)]. The "unexpected" transition is attributed to (unaccounted by) random perturbations in the wave loadings. Random noise components thus need to be incorporated in the analytical models despite the fact that the physical structural system is designed to behave in a deterministic manner in the experiment (Yim et al. 1993). Accordingly, analytical theory and numerical results are developed in Part I to identify and analyze the effects of weak random noise on periodically driven nonlinear moored structures. Specifically, noisy nonlinear responses are examined via a global stability analysis (Melnikov process) as well as a probabilistic analysis procedure (Fokker-Planck equation). As a result, complex responses, including noisy chaos, and rich nonlinear phenomena, such as bifurcations and coexisting response attractors, are demonstrated from a stochastic perspective. Strange chaotic attractors and their fractal details, and coexisting attractors and their relative strengths are clearly portrayed by the corresponding probability density functions in phase space shown in Part I.

This paper (Part II) presents an experimental study of stochastic properties of nonlinear moored structural responses subjected to noisy monochromatic wave excitations. The objective is threefold: (1) To validate the analytical model derived in Part I; (2) to present an experimental investigation of the noise effects on nonlinear moored structural responses; and (3) to assess the possible existence of chaotic response in noisy environments, including field conditions.

Setup and configurations of the stochastic experiment closely follow its deterministic counterpart (Lin et al. 1998), and the wave excitations are designed to incorporate the presence of weak random noise components. Experimental results are classified and demonstrated based on their nonlinear and stochastic properties and are used to verify the analytical and numerical predictions presented in Part I. Parameters of the analytical model are identified based on the experimental data. The analytical model is validated by comparing the simulated and experimental results. Poincaré points (sampled every forcing excitation period) are used to demonstrate the coexistence of multiple attractors and the interattractor transitions among the competing steady-state responses.

SYSTEM DESCRIPTION

The multipoint moored structural system considered in this study is formulated as a single-degree-of-freedom (SDOF) submerged rigid body, hydrodynamically damped, and excited nonlinear oscillator with random perturbations.

Model Configuration

The configuration of the experimental model consisted of a sphere on a rod that was supported by guyed masts 6 ft above the bottom of the wave flume (Fig. 1). The PVC sphere of 18-in. diameter was submerged and filled with water. The sphere weighed (in air) 25 lb empty and 106 lb filled. The rod restrains free play of the sphere, thus the model behaves as an SDOF system in surge. Two Delrin bearings were placed on the sphere to minimize the friction between the sphere and the rod. The 90° configuration (geometry parameter $\beta = 0$ in Part I), with the highest degree of nonlinearity in the restoring force, was chosen for its rich, complex, nonlinear phenomena. Two springs of stiffness 20 lb/ft were then attached to the sphere at angles of 90° to provide a nonlinear restoring force. Initial tension in each spring was set at 25 lb to ensure the model response frequently reaching the nonlinear regime.

[1]Prof., Dept. of Civ. Engrg., Oregon State Univ., Corvallis, OR 97331.
[2]Res. Assoc., Dept. of Civ. Engrg., Oregon State Univ., Corvallis, OR.

Note. Discussion open until November 1, 2000. To extend the closing date one month, a written request must be filed with the ASCE Manager of Journals. The manuscript for this paper was submitted for review and possible publication on May 9, 1996. This paper is part of the ***Journal of Waterway, Port, Coastal, and Ocean Engineering***, Vol. 126, No. 3, May/June, 2000. ©ASCE, ISSN 0733-950X/00/0003-0113–0120/$8.00 + $.50 per page. Paper No. 13219.

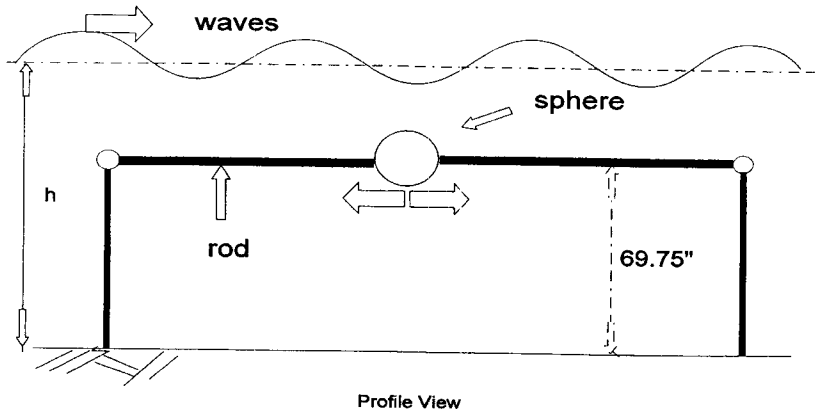

FIG. 1. SDOF Experimental Model Subjected to Monochromatic Waves with Random Perturbations

Equations of Motion

The response behavior of a periodically driven moored structure with random perturbations can be modeled by the following set of first-order nonlinear ordinary differential equations (Yim et al. 1993):

$$\dot{x}_1 = x_2$$

$$\dot{x}_2 = \frac{1}{(M + M_a)} [-R(x_1) - \gamma x_2 + F_D(x_2) + F_I(x_1, x_2) + \zeta(t)] \quad (1a)$$

where x_1 and x_2 = surge displacement and velocity, respectively; M = sphere mass; M_a = added mass; and γ = structural damping coefficient. R = system restoring force (due to nonlinear geometric configuration), which is given by

$$R(x_1) = \alpha \left[x_1 - \tau \left(\frac{l_1 + l_2}{l_1 l_2} x_1 \right) \right] \approx k_1 x_1 + k_3 x_1^3$$

$$l_{1,2} = (1 + x_1^2)^{1/2} \quad (1b)$$

where α = stiffness parameter; and τ = parameter of initial tensions in the mooring lines. Good agreement between the taut mooring restoring force and a two-term polynomial approximation [(1*b*)] in the response range considered has been demonstrated by Gottlieb and Yim (1993). F_D denotes the drag force and is given by

$$F_D = \frac{1}{2} \rho C_d A_p (u - x_2)|u - x_2| \quad (1c)$$

where ρ = water density; C_d = drag coefficient; A_p = projected area; and u = fluid particle velocity. F_I represents the inertial force and is given by

$$F_I = \rho C_m \forall \frac{\partial u}{\partial t} \quad (1d)$$

where C_m = inertial coefficient; and $\forall$ = sphere volume. The stochastic excitation component is described by a band-limited noise perturbation $\zeta(t)$ incorporating all possible randomness in the wave field. Note that in Part I, the random perturbations are approximated by an ideal white noise for the convenience of Fokker-Planck formulation and demonstration. The Rice noise (band-limited) representation used in Melnikov analysis in Part I is chosen here to provide a practical noise model. The simulated structural response will be used to compare with experimental data in a later section. The perturbation component $\zeta(t)$ is given by

$$\zeta(t) \cong \sum_{j=1}^{N} a_j \cos(\omega_j t - \varphi_j) \quad (2)$$

where φ_j = uniformly distributed independent random variable in the interval of $[0, 2\pi)$.

Setup and Data Acquisition

The experimental model shown in Fig. 1 was positioned in a 2D wave flume of length 342 ft, width 12 ft, and depth 15 ft. Waves were generated by oscillatory motions of a hydraulically driven, hinged-flap wave board (maximum strokes at ±30 in.). A VAX 3400 server and two VAX 3100 stations with optical communication links were used for wave generation control and 64 channels of digital data acquisition (Yim et al. 1993). Digital data recorded during each test included wave profiles at several locations along the channel, current and sphere movements, and restoring forces in the springs.

To measure the wave profile, three resistive wave gauges were placed on each side of the model at distances of 1.5, 4.0, and 11.0 ft from the model. A current meter was placed 10 in. upstream of the model, 22 in. from the sidewall at a depth of 9 in. Two string pots were used to measure the displacement of the sphere. The string pots were attached to the sphere on opposite sides to offset the force caused by the string pots. Another two string pots measuring the elongation of the springs were used to determine the restoring forces. Monochromatic waves with random perturbations were generated based on given energy spectrum densities with designed noisy intensities.

Each test was performed sufficiently long to ensure that the transient response damps out. Data acquisition tests were initially performed over a range of frequencies and wave heights at which interesting nonlinear responses may be expected based on the deterministic testing data. In the deterministic tests, the model with the 90° configuration ($\beta = 0$) subjected to 2 ft, 2 s waves exhibited subharmonic nonlinear behavior. The wave period of 2 s was selected for all tests, and the wave amplitudes varied within the range of 1.5–2.5 ft. The random noise variance was designed to range within 15% of the total input energy.

Observations and Discussions

A primary goal of this experimental investigation is to examine the effects of weak random perturbations in the exciting waves on the highly nonlinear model responses and possible routes to chaos. It is noted that the excitation conditions in Part I for chaotic responses are beyond the capacity of the laboratory facilities. The wave height corresponding to chaotic structural responses exceeds 100 ft (converted from nondimensionalized version, cf. Fig. 5 in Part I), which is far out of the scale of the 15-ft-deep wave tank. Nevertheless, possible noisy chaotic model response in a lower excitation range is observed. The response will be examined and discussed in

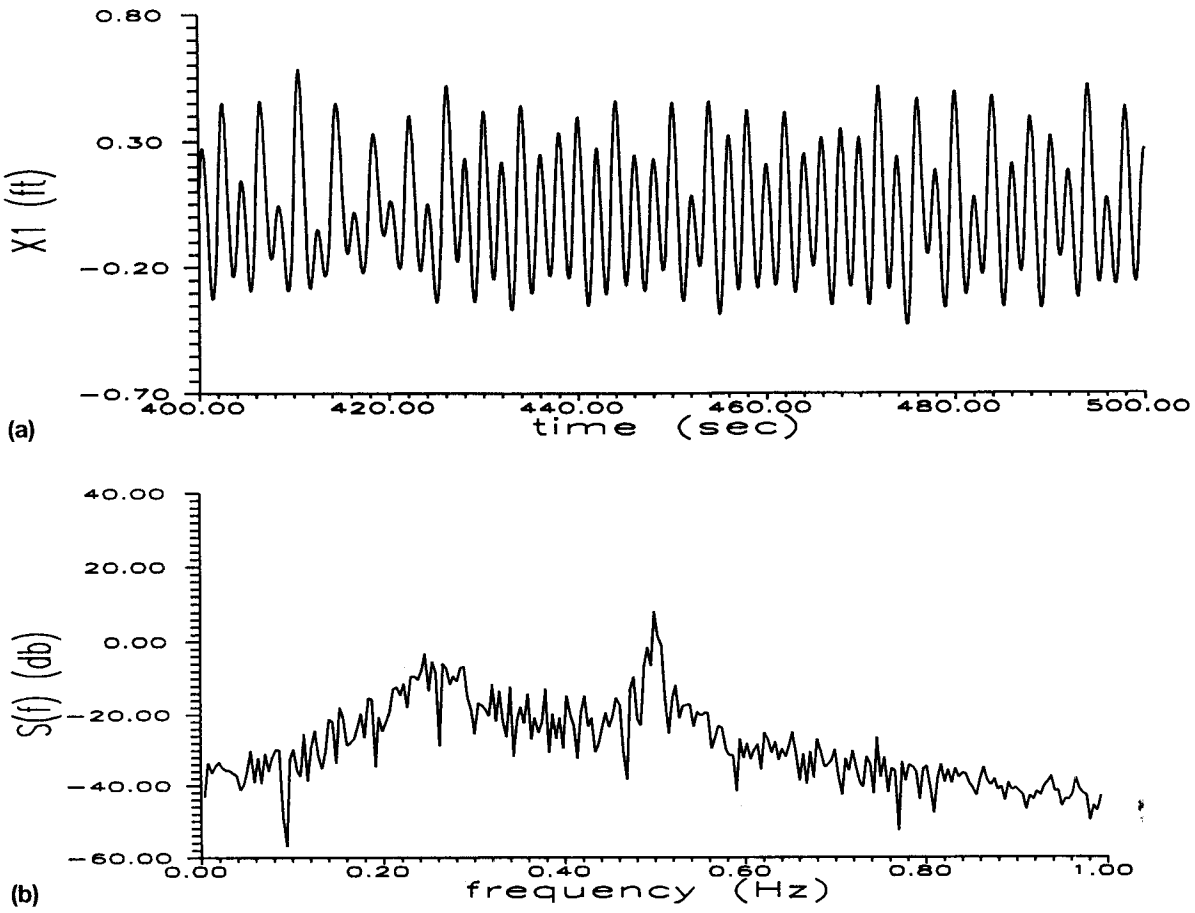

FIG. 2. Noisy Harmonic Response (Test D10): (a) Time History; (b) Energy Spectrum

later sections. Moreover, within the capacity of the facility, experimental results appear closely in line with the analytical predictions presented in Part I in overall response behavior. More detailed analysis of the experimental results including noise-induced transitions and noise effects on system performance also will be discussed.

Under the specified wave excitation conditions described above, a total of nine tests were conducted and the model responses were recorded [Tests D4–13, see Yim et al. (1993) for detailed documentation]. Figs. 2 and 3 (Tests D10 and D11, respectively) show sample model responses in the time history and energy spectrum. Diminutive energy content in the subharmonic frequency range is observed for Test D10 [Fig. 2(b)]. The model response is harmonically dominated, but subharmonic characteristics are indeed present and easily identified. When the wave amplitude is increased from 1.5 ft (Test D10) to 2.2 ft (Test D11), a relatively strong subharmonic component is observed in the response in both the time and frequency domains (Fig. 3). It is evident that the response oscillates between the two coexisting distinct response attractors, i.e., harmonic and subharmonic (Fig. 3). The experimental observation can be interpreted in light of the analytical prediction in Part I, which suggests that the presence of random noise facilitates a global description of the system behavior in the phase space. When the random noise intensity is moderate, the attraction domains of the coexisting responses are well-bridged. The steady-state probability density function indicates an oscillatory shift between coexisting response attractors in an ensemble sense (cf. Fig. 3, Part I). Drifting of the experimental response back and forth between the coexisting harmonic and subharmonic attractors is caused by the presence of random noise, and the combined characteristics are observed (Fig. 3).

VALIDATION OF ANALYTICAL MODEL

Identification of Noise Intensity and System Parameters

This experimental study is also designed to validate the analytical model governing the randomly perturbed nonlinear moored structural responses presented in Part I. The presence of random and uncontrollable components in the wave excitation is incorporated in the analytical model as a linearly filtered noise as shown in (2). Experimental observations indicate that besides the designed (analytically specified) band-limited noise component, there exist additional, uncontrollable "random" perturbations due to imperfections in the wave generation and bounded wave field. The effects of these imperfections (caused by diffractions, reflections, and return currents in the wave flume), together with the analytically specified noise intensity in the waves, needs to be directly computed from the experimental data.

The time history of a wave profile $y_m(t)$ from the experiment can be written as superposition of a deterministic sinusoidal signal $y_d(t)$ and a random portion $\zeta(t)$

$$y_m(t) = y_d(t) + \zeta(t) = A \cos \omega t + \zeta(t) \tag{3a}$$

where subscripts m and d denote measured and deterministic, respectively. The record of $y_m(t)$ is then divided into N segments of equal length $y_{m1}(t)$, $y_{m2}(t)$, . . . , $y_{mNe}(t)$ and the ensemble-averaged time series $y_e(t)$ can be estimated

$$y_e(t) = \sum_{i=1}^{N_e} \left[\frac{1}{N} \sum_{j=1}^{N} y_{mj}(t) \delta(t - t_i) \right] \tag{3b}$$

where subscript i denotes the ith time step and N_e the number of ensembles, and

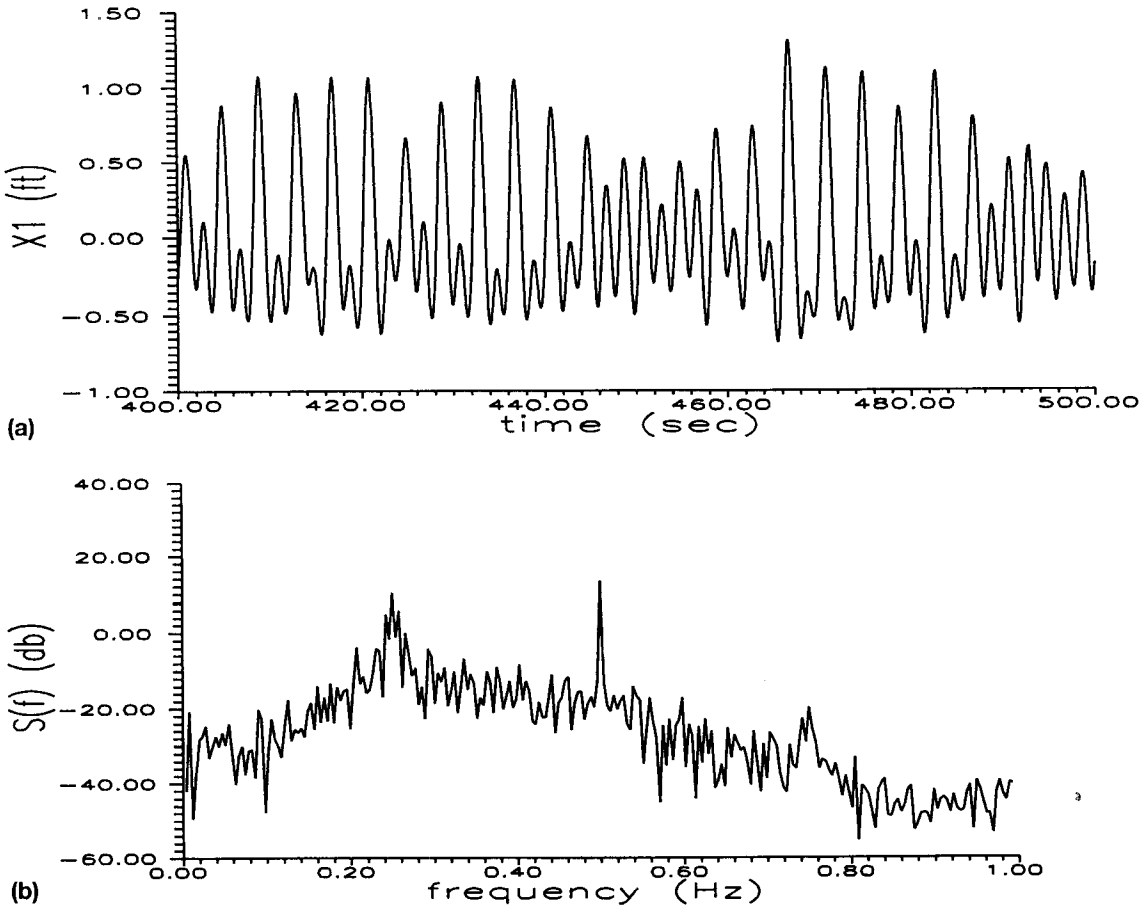

FIG. 3. Noisy Subharmonic Response (Test D11): (a) Time History; (b) Energy Spectrum

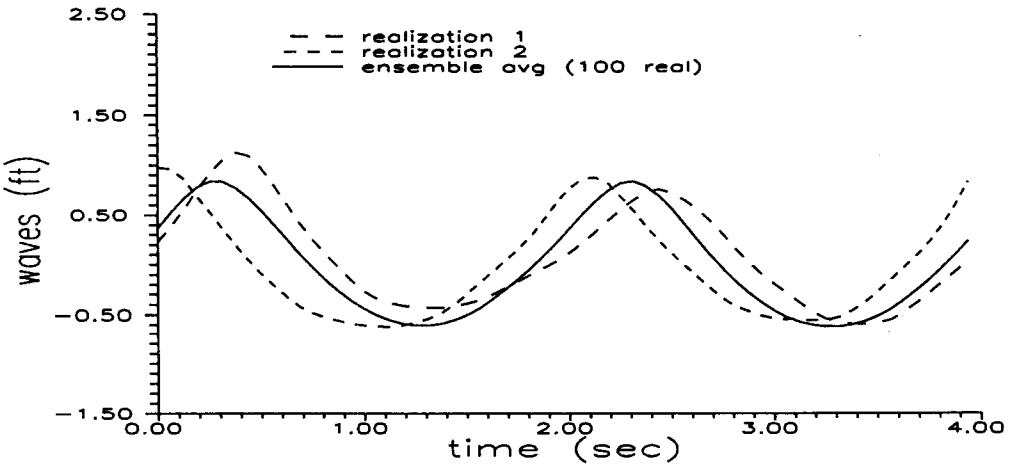

FIG. 4. Identifying Deterministic Component from Noisy Periodic Waves (Test D11)

$$y_e(t_i) = \frac{1}{N}\sum_{j=1}^{N} y_{mj}(t_i) \cong E[y_m(t_i)] = E[y_d(t_i)]$$

$$+ E[\zeta(t_i)] \cong y_d(t_i) \tag{3c}$$

Adjusting the wave time history to zero-mean, and assuming $y_d(t)$ and $\zeta(t)$ are uncorrelated, the variances of the waves are given by

$$\text{var}(y_m) = \text{var}(y_d) + \text{var}(\zeta) = \frac{A^2}{2} + \sigma_\zeta^2 \cong \text{var}(y_e) + \sigma_\zeta^2 \tag{3d}$$

The noise intensity can then be estimated by

$$\sigma_\zeta^2 = \text{var}(y_m) - \text{var}(y_e) \tag{3e}$$

Fig. 4 shows an example of isolated deterministic components from noisy periodic waves (Test D11). The time history of the wave profile is divided into 100 segments, and the "ensemble average" time history is obtained by applying the above procedure. The noise variance is identified to be 10% of the total input energy.

Identification of system parameters M, M_a, γ, C_d, k_1, and k_3 of the analytical model is conducted utilizing the model configurations, results of free vibration tests, and a reverse multiple-input/single-output technique (Bendat and Piersol 1993).

Based on the response amplitude ranges, stiffness coefficients are calculated using a least-squares approximation to the spring configurations. Free vibration tests provide an initial guess for structural damping coefficient (Yim et al. 1993). The

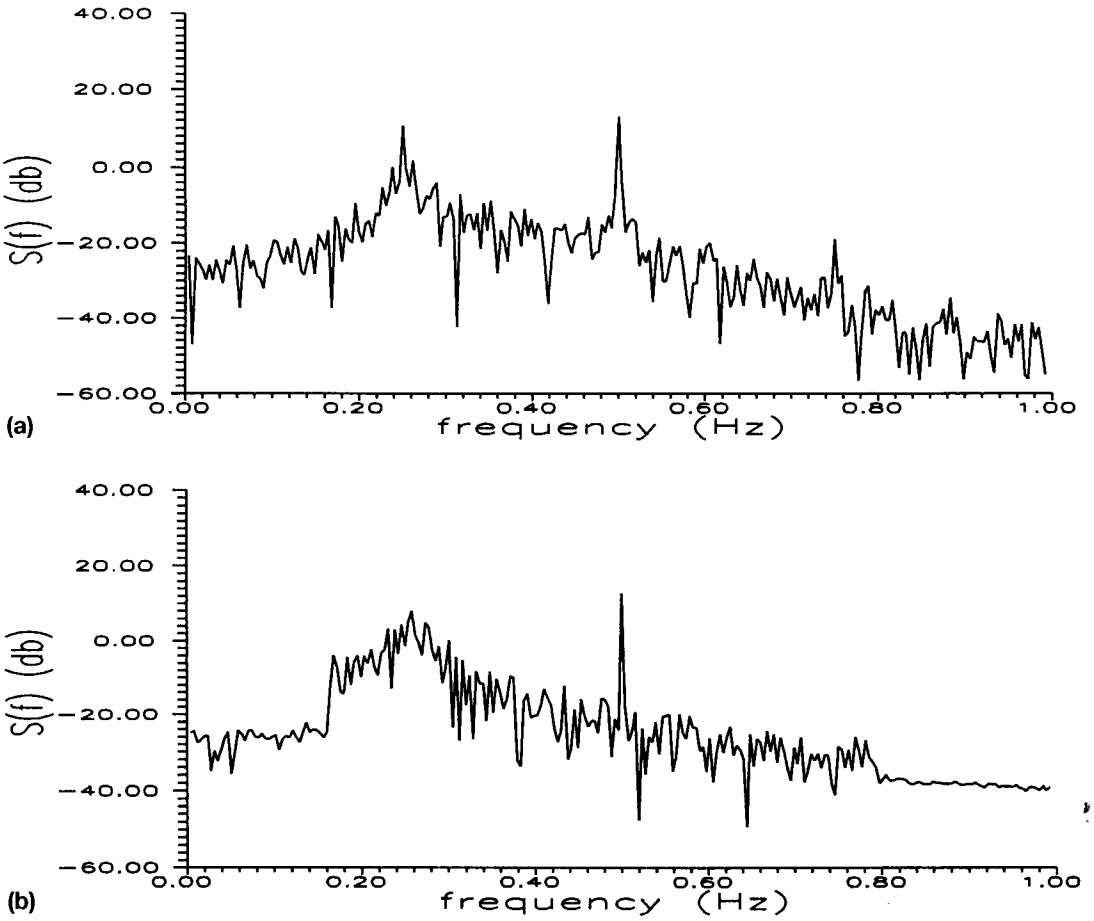

FIG. 5. Noisy Subharmonic Response (Test D12), Energy Spectrum: (a) Measured Data; (b) Simulated Results

total energy dissipation mechanism, including structural, hydrodynamic, and Coulomb friction, is represented by an equivalent linearized damping. Following the standard linear analysis to compute the critical damping coefficient based on the mass and stiffness of the equivalent linear system, the structural damping can be identified. The reverse multiple-input/single-output technique identifies the system's natural frequency and provides an initial guess for drag and added mass coefficients in the frequency domain. In this technique, the roles of inputs and outputs are interchanged, and the reversed system is linear in nature (Bendat and Piersol 1993). Following the identification procedure, the measured wave excitations are treated as outputs to the reverse system and structural responses as inputs. Applying the standard linear analysis procedure to the reversed system, system parameters can be identified in the frequency domain. The structural damping, drag, and added mass coefficients estimated by applying the above procedure are later fine-tuned via numerical simulations.

Fig. 5 illustrates a comparison of the measured response data (Test D12) and simulated results. For the simulation, the wave profile constitutes a dominant periodic component and band-limited random perturbations with the variance computed from the experimental data. Parameters of the analytical model are estimated using the above procedure and then optimized by fitting the simulated and experimental results with respect to amplitude and phase. Good agreement in the responses is shown in the frequency domain (Fig. 5). Note that the energy dissipation mechanism of the analytical model is represented by a structural damping and Morison drag, which may not fully capture the effects due to hydrodynamics and the time-varying Coulomb friction. Nevertheless, the good match shown in Fig. 5 indicates that the model is appropriate for the response range considered.

DATA ANALYSIS

The above investigation demonstrates the nonlinear, stochastic nature in the experiment model response and also the validity of the analytical model proposed in Part I (within the response range considered via a finite number of experimental data sets). A detailed analysis of the data on the noise-induced interdomain transitions and the noise effects on the response characteristics and system performance is shown in the following sections.

Noise Effects on Single Attractor and Multiple Coexisting Attractors

When the moored structural system is deterministically excited, the backbone curve in the associated frequency response diagram indicates the locations of stability regions (Lín and Yim 1995). The structure may oscillate within a single response attractor or coexisting multiple attractors, depending on excitation details and initial conditions (Lin and Yim 1995). It is also analytically predicted that, with the presence of weak noise among coexisting multiple attractors, response trajectories may transition from one attractor to another (Lin and Yim 1997). As mentioned, besides the designed additive random perturbations, there is weak uncontrollable tank noise present in the wave excitation. Distinct effects by noise perturbations of various intensities on experimental responses of a single attractor or multiple coexisting attractors are demonstrated in this section.

Fig. 6(a) shows the time history of an experimental "designed" deterministic response (Test D1) with system parameters and excitation details in the stability region of a single attractor. Small variations in the response amplitude caused by the weak tank noise are noted to oscillate along its determin-

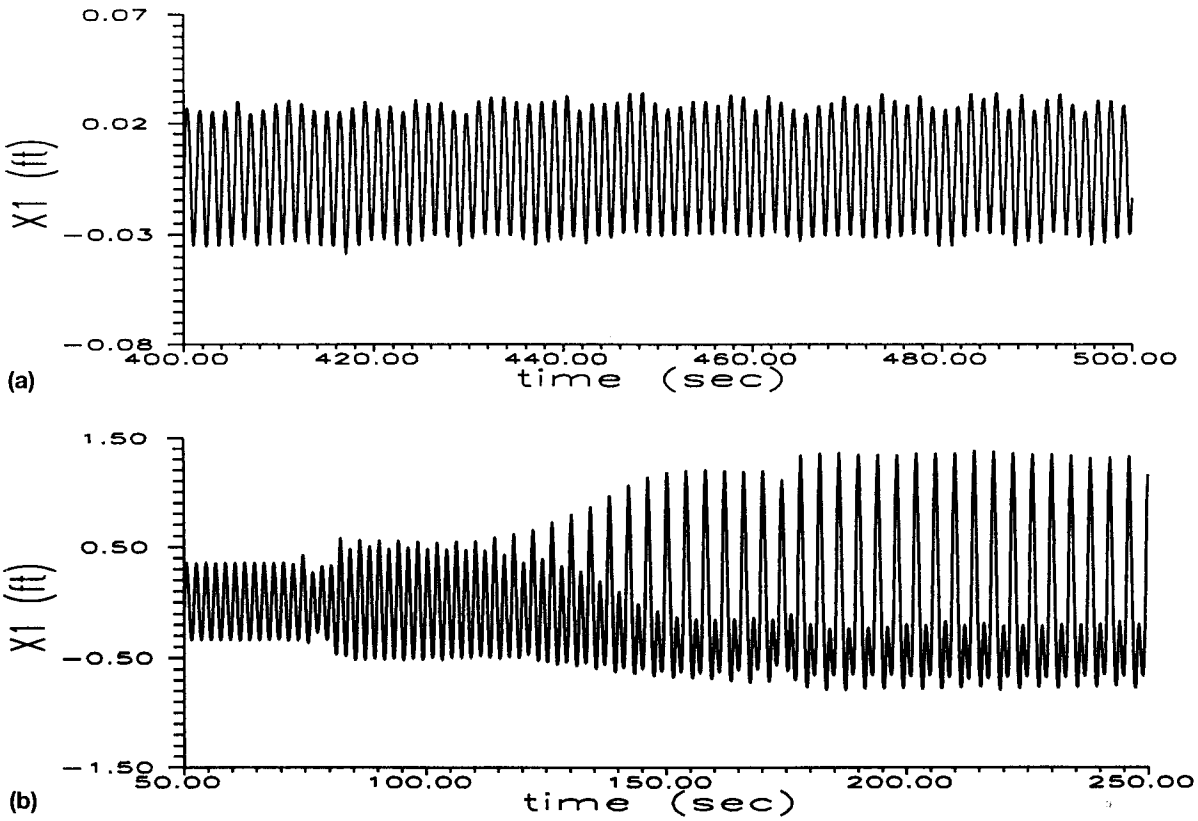

FIG. 6. Time Histories of Model Response with Presence of Weak Tank Noise Perturbations: (a) Single Attractor Response (Test D1); (b) Two Coexisting Attractor Responses (Test D2)

istic counterpart. Fig. 6(b) shows a time history of a designed deterministic model response (Test D2) with system parameters and excitation details in the stability region of multiple coexisting attractors. The response is observed to stay in a harmonic fashion for about 120 s and then to transition to a subharmonic mode. It verifies the analytically predicted transition phenomenon caused by the presence of weak noise presented in Part I. Because the transition phenomenon is of major interest, the noise level is increased to further examine its effects on the response when multiple coexisting attractors are present.

Fig. 7 shows the time histories of model responses with two coexisting attractors to random perturbations with moderate intensities. It is observed that the response attractors are well-bridged due to the presence of designed noise perturbations. The response trajectory oscillates between harmonic and subharmonic modes as shown in Fig. 7(a). The transition phenomenon becomes more pronounced as the noise intensity increases. When the noise intensity becomes large [Fig. 7(b)], the corresponding response time history becomes more random-like. The individual harmonic and subharmonic attractors can barely be traced, which verifies the overall noise effects on nonlinear structural responses predicted in Part I.

Noise-Induced Transitions

As demonstrated in the analytical predictions presented in Part I and verified by experimental observations (Fig. 7), the presence of noise, indeed, bridges coexisting response attractors (two attractors in these cases). Morever, there are cases that multiple steady-state responses coexist and are bridged by the presence of noise. An example of four coexisting attractors is shown below in which one of the attractors observed appears to exhibit noisy chaotic behavior. Analysis on the characteristics of these attractors, and the associated interattractor oscillatory transitions, are examined here in more detail.

The experimental responses are sampled and examined on a Poincaré section. A Poincaré point is sampled at time interval of forcing excitation period to suppress periodicity due to the dominant periodic excitation component. A Poincaré map is formed by a collection of Poincaré points. Concentration of Poincaré points on the section indicates the corresponding attractors.

Fig. 8(a) shows the Poincaré map of a sample experimental model response (Test D13). The scattering of the points implies either noise-bridged multiple coexisting response attractors or a single noisy chaotic attractor (cf. Part I). In this case, a Poincaré time history of the response (Poincaré points versus time) may better reveal the response characteristics. Fig. 8(b) shows that there are transitions among different steady states. Specifically, there are seven transitions occurring at around the 300th, 425th, 550th, 1,175th, 1,450th, 1,575th, and 1,700th s, respectively. The Poincaré time history is accordingly divided into eight segments [I–VIII in Fig. 8(b)]. A single attractor is assumed to be embedded in each response segment, and transitions from one attractor to another are attributed to the presence of noise.

For further comparison and investigation of these attractors, a Poincaré map is constructed for each individual attractor (or time segment). Attractors of similar shape and location are deemed identical, and revisiting of the response trajectory to the attractor is indicated. It is shown that the attractors embedded in each of the pairs of Segments I and V, II and VI, III and VII, and IV and VIII appear to be identical (and are not presented here due to length limitation). Analysis results indicate that there are four coexisting response attractors embedded in the response time history of Test D13, and they are bridged by the presence of the random noise. It is noted that the attractor embedded in Segments IV and VIII shows structured spreading that resembles the shape of the full-length data [cf. Fig. 8(a)], and is suspected to be noisy chaotic. Spectral analysis and Lyapunov exponent calculation have been applied to these attractors (with special interest in Segments IV and

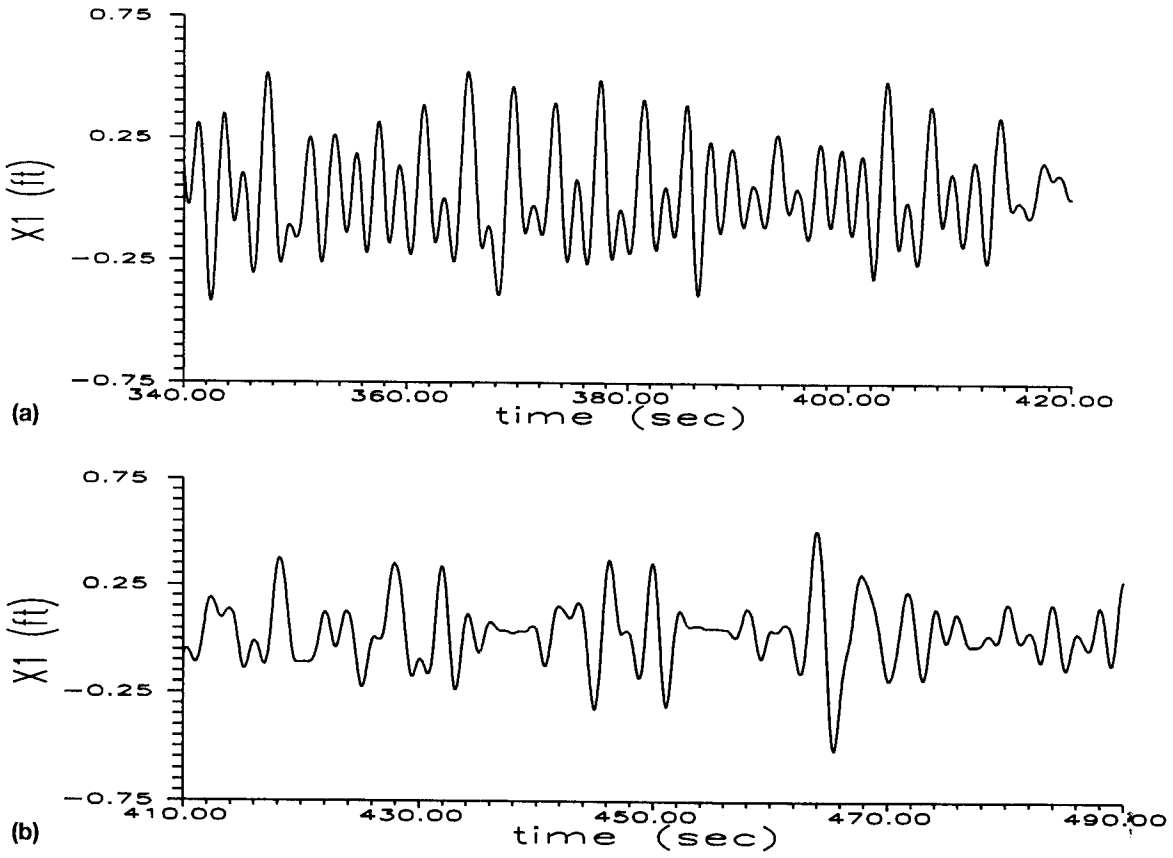

FIG. 7. Time Histories of Two Coexisting Attractor Model Responses to Various Noise Intensities: (a) Test D8($\sigma_\zeta^2 \cong 0.02$); (b) Test D6 $\sigma_\zeta^2 \cong 0.04$)

VIII) in an attempt to quantitatively identify noisy chaos. However, due to the fact that the responses are perturbed by a relatively strong noise, no definite conclusions can be made with quantitative evidences at this point.

The degree of nonlinearity and characteristic behavior of each embedded response attractor is yet to be identified and classified. Techniques of extracting response attractors from strongly noisy time histories are to be applied to isolate the attractors, and also more advanced data analysis techniques are needed to classify each nonlinear response attractor with finite, limited data length.

Assessment on Existence of Noisy Chaos

No quantitative evidence is yet available to draw definite conclusions on the existence of noisy chaotic model responses to moderate noise perturbations (e.g., Test D13). Nonetheless, based on the observations of experimental results and the associated Poincaré maps, the possible existence of chaotic response in noisy environments is discussed here.

As mentioned previously, a reason that no definite steady-state chaotic responses have been achieved and positively observed in the experiment is due to the fact that the wave conditions corresponding to chaos in the analytical prediction are out of the scale of the wave tank facility. Another reason may be concluded based on the analysis of the result of Test D13. It is shown that the presence of noise bridges coexisting and competing response attractors, and the response trajectory drifts in and out of their attracting domains. Noisy chaotic characteristics may actually have been exhibited in brief durations over various segments of a single response time history. However, as indicated analytically, the strength of the chaotic attractor of the moored structure is relatively weak compared to its coexisting periodic counterparts, thus the phenomenon may not be discernable. More efforts should be devoted in analyzing and classifying the transition, recurring behavior of noisy nonlinear (possibly chaotic) responses in future studies. However, from an engineering application viewpoint, chaos is a motion of finite amplitude, and its unpredictability and randomness become less significant in noisy environments. Comparatively, large excursions in model responses may cause more servere damage to the structure considered.

CONCLUDING REMARKS

This study presents experimental observations, analytical model validation, and analysis of experimental results of a moored, submerged structural system with hydrodynamic and geometric nonlinearities subjected to monochromatic wave excitation with random perturbations. Based on the results presented, the following concluding remarks are in order:

- Noisy nonlinear structural oscillations, including harmonic, subharmonic, and possibly chaotic responses are experimentally observed.
- System parameters of the proposed analytical model in Part I are identified by using a procedure incorporating model geometric configuration, modern system identification technique, and numerical simulations. Good agreement between experimental data and simulated responses is demonstrated, thus validating the analytical prediction model.
- Noise effects are examined on nonlinear model responses with a single attractor and multiple coexisting attractors.

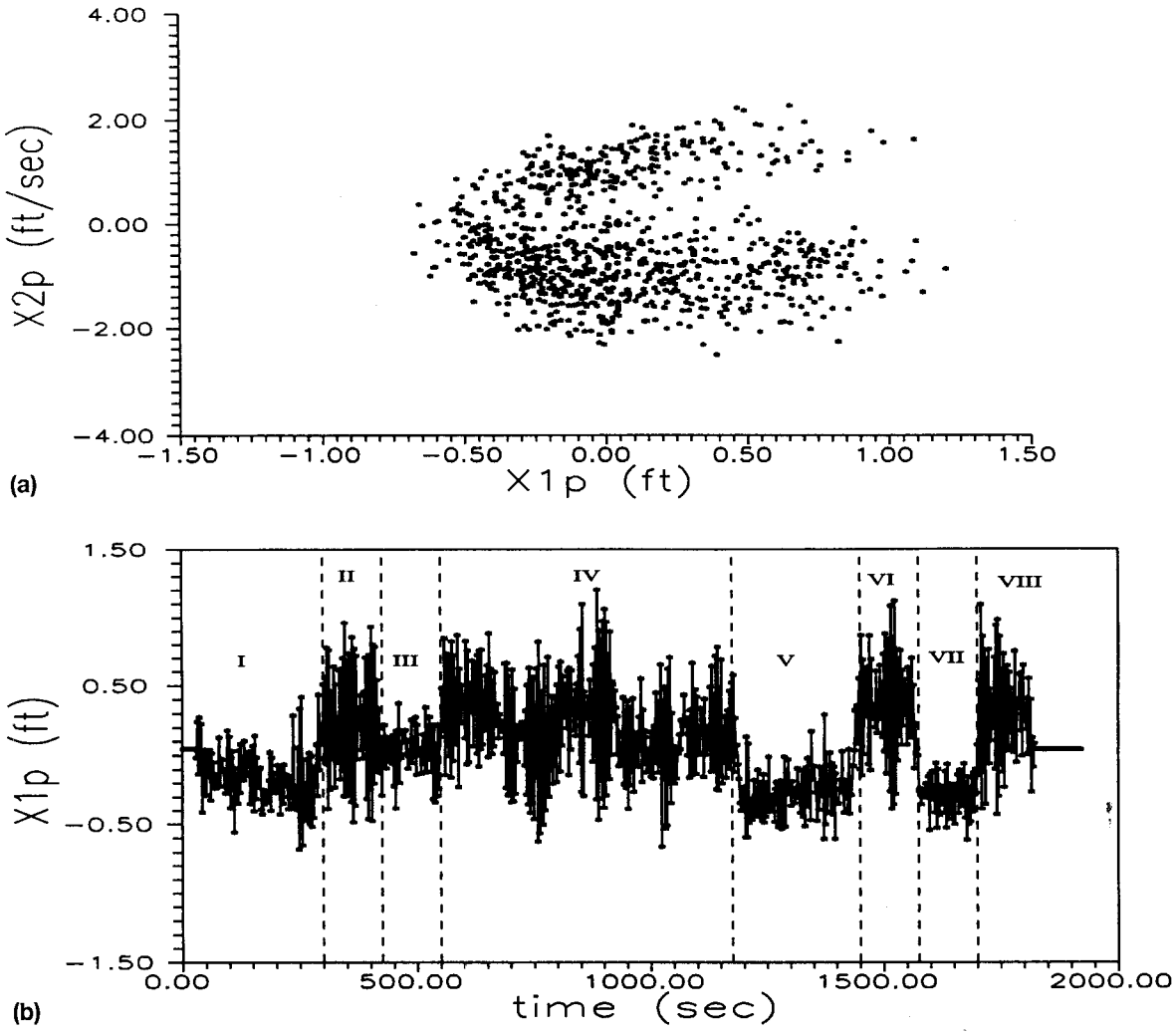

FIG. 8. Poincaré Analysis of Response of Test D13: (a) Poincaré Maps; (b) Poincaré Points versus Time

For the single attractor responses, the presence of a weak noise causes fluctuations in the amplitude along their deterministic counterparts. For multiple coexisting attractor responses, the presence of very weak perturbations (tank noise) drives the response trajectory from the weaker attractor to the stronger ones. Under moderate noise intensity, the multiple coexisting attractors are well-bridged. Combined response characteristics can be observed over various segments of a single time history.

- Possible, albeit brief, noisy chaotic responses are observed to be embedded in an experimental result with multiple coexisting attractors. Due to its weak strength compared to other coexisting, competing periodic attractors, chaotic responses are assessed likely to be embedded in short time segments of a single noisy time history. This may provide an indicator to identify chaotic response from field data.

ACKNOWLEDGMENT

The writers gratefully acknowledge the financial support from the U.S. Office of Naval Research (Grant No. N00014-92-J-1221).

APPENDIX. REFERENCES

Bendat, J. C., and Piersol, A. G. (1993). *Engineering applications of correlation and spectral analysis*. Wiley, New York.

Gottlieb, O., and Yim, S. C. S. (1992). "Nonlinear oscillations, bifurcations and chaos in a multi-point mooring system with a geometric nonlinearity." *Appl. Oc. Res.*, 14, 241–257.

Gottlieb, O., and Yim, S. C. S. (1993). "Drag-induced instability and chaos in mooring systems." *Oc. Engrg.*, 29, 569–599.

Gottlieb, O., Yim, S. C. S., and Lin, H. (1997). "Analysis of bifurcated superstructure of nonlinear ocean system." *J. Engrg. Mech.*, ASCE, 123(11), 1180–1187.

Lin, H., and Yim, S. C. S. (1995). "Chaotic roll motion and capsizing of ships under periodic excitation with random noise." *Appl. Oc. Res.*, 17. 185–204.

Lin, H., and Yim, S. C. S. (1997). "Noisy nonlinear motions of moored system. Part I: Analysis and simulations." *J. Wtrwy., Port, Coast., and Oc. Engrg.*, ASCE, 123(5), 287–295.

Lin, H., Yim, S. C. S., and Gottlieb, O. (1998). "Experimental investigation in bifurcations of an ocean system." *Oc. Engrg.*, 25(4/5), 323–343.

Yim, S. C. S., Myrum, M. A., Gottlieb, O., Lin, H., and Shih, I.-M. (1993). "Summary and preliminary analysis of nonlinear oscillations in a submerged mooring system experiment." *Rep. No. OE-93-03*, Oc. Engrg. Program, Oregon State University, Corvallis, Oreg.